Allosteric Effects of RuvA Protein, ATP, and DNA on RuvB Protein-Mediated ATP Hydrolysis†

Paul E. Marrione and Michael M. Cox*

Department of Biochemistry, College of Agriculture and Life Sciences, University of Wisconsin, Madison, Wisconsin 53706

Received February 9, 1996; Revised Manuscript Received May 20, 1996⊗

ABSTRACT: A detailed characterization of RuvB protein-mediated ATP hydrolysis in the presence of RuvA protein has provided (a) the steady-state kinetic parameters of ATP hydrolysis within a RuvAB complex and (b) several insights into the mechanism of ATP hydrolysis and its coupling to translocation on DNA. In general, the RuvA protein increases the k_{cat} and decreases the K_m for the RuvB ATPase activity. DNA has a much greater effect on the kinetics of ATP hydrolysis when RuvA is present, consistent with a role of RuvA in facilitating the interaction between RuvB and DNA. Mechanistic clues come from deviations from normal steady-state kinetic behavior. A previously described burst of ATP hydrolysis, corresponding to two ATPs per RuvB hexamer [Marrione & Cox (1995) *Biochemistry 34*, 9809−9818], is still observed in the presence of RuvA protein. This suggests a functional asymmetry in the RuvB hexamer. There is a gradual attenuation of ATP hydrolysis when RuvB protein, alone or in the presence of RuvA protein, hydrolyzes ATP at ATP concentrations below the K_m. The attenuation is observed even though an ATP regeneration system is present. ATP hydrolysis simply halts after a limited number of turnovers. The attenuation is reversible, and the effects of RuvA protein, DNA, and additional ATP in reversing the effect provide evidence for a complex array of allosteric interactions operating within the RuvB hexameric helicase. We propose a model in which individual subunits in a RuvB hexamer are functionally paired, with the three pairs moving sequentially and cooperatively through a multistep ATP hydrolytic cycle.

The RuvA and RuvB proteins of *Escherichia coli* process branched DNA intermediates created by the action of RecA protein at a late stage of recombinational DNA repair and homologous genetic recombination (Shinagawa et al., 1991; West & Connolly, 1992; Kuzminov, 1993; West et al., 1993; Müller & West, 1994). In vitro, these proteins possess a DNA helicase activity (Tsaneva et al., 1993; Tsaneva & West, 1994) and promote a rapid branch migration of Holliday junctions (Iwasaki et al., 1992; Tsaneva et al., 1992b; Lloyd & Sharples, 1993). The helicase activity is believed to be mechanistically related to the promotion of branch migration and the processing of branched DNA molecules in which branch migration is blocked by heterologous DNA sequences (Iype et al., 1994, 1995; Müller & West, 1994; Tsaneva & West, 1994).

DNA helicases are oligomeric proteins that fall into at least two structural classes, functioning as either hexamers (Dean & Hurwitz, 1991; Dean et al., 1992; Geiselmann et al., 1992a,b; Geiselmann & von Hippel, 1992; Bujalowski et al., 1994; Dong et al., 1995; Egelman et al., 1995) or dimers (Lohman, 1992, 1993; Wong et al., 1992; Wong & Lohman, 1992). The RuvB protein functions as a hexamer of identical subunits (Mitchell & West, 1994; Stasiak et al., 1994). DNA helicases must translocate as they unwind DNA, and both the translocation and DNA unwinding are somehow coupled to the hydrolysis of ATP. Models for translocation and unwinding are linked closely to the oligomeric structure of helicases (Lohman, 1993). A detailed understanding of the interaction of all the sites of the RuvB hexamer with DNA and ATP will be critical to determine its mechanism of action in processing recombination intermediates.

The primary structure of the RuvB protein features at least one consensus ATP binding fold (Benson et al., 1988; Shinagawa et al., 1988). The RuvB protein hydrolyzes ATP in a DNA-stimulated manner (Shiba et al., 1991; Müller et al., 1993b; Mitchell & West, 1994; Marrione & Cox, 1995). The helicase and branch migration activities are both dependent on the hydrolysis of ATP by RuvB protein (Parsons et al., 1992; Tsaneva et al., 1992b, 1993). The RuvA protein facilitates the binding of RuvB protein to DNA (Müller et al., 1993a), and is required for the helicase function (Tsaneva et al., 1993). The RuvA protein has been reported to stimulate the ATPase activity of the RuvB protein (Tsaneva et al., 1992b; Mitchell & West, 1994), but the kinetic effects of RuvA have not been investigated in detail.

The ATPase activity of the RuvB protein alone was characterized previously (Marrione & Cox, 1995), including the effects of DNA cofactors. In this report, we build on these observations by examining the effect of the RuvA protein on all aspects of RuvB protein ATPase activity.

MATERIALS AND METHODS

Enzymes and Reagents. *Escherichia coli* RuvA and RuvB proteins were purified as described below. Molecular biology grade Tris buffer was obtained from Fisher Scientific. Pyruvate kinase, lactate dehydrogenase, reduced β-nicotinamide adenine dinucleotide (NADH), phosphoenolpyruvate (PEP), bovine serum albumin (BSA), adenosine 5′-triphosphate (ATP), ultra-pure potassium glutamate, and all molecular biology grade salts were from Sigma Chemical Co. The purity of ATP was checked by thin-layer chromatography and was shown to be at least 99% pure, with the major

† This work was supported by Grant GM52725 from the National Institutes of Health. P.E.M. was supported in part by NIH Predoctoral Training Grant GM07215 and a Wharton Fellowship.

* Corresponding author. Phone: 608-262-1181. Fax: 608-265-2603. Email: COXLAB@MACC.WISC.EDU.

⊗ Abstract published in *Advance ACS Abstracts,* August 15, 1996.

S0006-2960(96)00316-9 CCC: $12.00

contaminant being ADP. The concentration of ATP was determined by the absorbance at 259 nm, using the extinction coefficient $\epsilon_{259} = 1.54 \times 10^4\ M^{-1}\ cm^{-1}$. [$\alpha$-^{32}P]ATP (3000 Ci/mmol) was from Amersham. Labeled ATP with greater than 5% ADP contamination was not used in experiments. DC-plastikfolien poly(ethylenimine)−cellulose f (PEI-cellulose) thin-layer chromatography sheets were purchased from EM Separations. Phosphocellulose P11 was from Whatman. Macroprep ceramic hydroxyapatite (type I) and DEAE Bio-gel A−agarose were purchased from BioRad. Restriction enzymes were from New England Biolabs, and topoisomerase I was from Gibco-BRL. Bradford protein concentration assays were carried out with the BioRad protein assay kit (BioRad).

The following buffers were prepared with deionized double-distilled water. TEGD buffer (used in the RuvB protein purification) is 20 mM Tris−acetate (80% cation), 1 mM EDTA,[1] 10% (v/v) glycerol, and 1 mM dithiothreitol. The final pH of TEGD after addition of all components is 7.7 at room temperature. RuvB protein storage buffer is 20 mM Tris−acetate (80% cation), 150 mM sodium acetate, 50% (v/v) glycerol, 1 mM dithiothreitol, and 0.02 mM EDTA. The final pH of this buffer is 7.6 at room temperature. P100 buffer, used for RuvA protein purification, is 100 mM potassium phosphate (51% dication), 10.0% (v/v) glycerol, 150 mM KCl, and 1.0 mM dithiothreitol. P600 buffer is the same as P100 except with 600 mM potassium phosphate. The final pH of the P buffers is 6.7 at room temperature. RuvA protein storage buffer is 20 mM Tris−acetate (80% cation), 50% (v/v) glycerol, 500 mM potassium glutamate, 2 mM dithiothreitol, and 0.02 mM EDTA (final pH 7.7 at room temperature). Buffer A, used in the experiments measuring the RuvB protein ATP hydrolytic activity in the presence of RuvA protein, is 20 mM Tris−acetate (80% cation), 10 mM magnesium acetate, 6.3% (w/v) glycerol, 2 mM dithiothreitol, and 100 μg/mL BSA (final pH 7.7 at room temperature). RuvAB dilution buffer contains 20 mM Tris−acetate (80% cation), 0.15 M NaOAc, 12.6% (w/v) glycerol, 1 mM EDTA, 0.5 mM dithiothreitol, and 100 μg/mL BSA (final pH 7.7).

Purification of the RuvB Protein. *E. coli* RuvB protein was purified as described (Tsaneva et al., 1992a; Iype et al., 1994) with the following modifications. The high-speed supernatant from the cell lysis was loaded onto a 485 mL phosphocellulose column (3.5 cm × 11 cm). The RuvB protein does not stick to this resin and elutes in the void volume (Tsaneva et al., 1992a; Iype et al., 1994). The RuvB-containing fractions were pooled and loaded onto a 240 mL (2.5 cm × 12 cm) DEAE-Biogel A column, equilibrated in TEGD. The column was washed once with 250 mL of TEGD and then once with 1 column volume of TEGD with 0.1 M potassium acetate (KOAc). The column was then developed with a 1.5 L linear gradient from 100 to 300 mM KOAc in TEGD. RuvB protein elutes between 180 and 240 mM KOAc. The rest of the procedure was as described except that the Biorex column was omitted from the procedure, and RuvB protein was dialyzed into a modified storage buffer as described above and stored at −70 °C. The final yield of RuvB protein from 13 g of cells was 250 mg. The RuvB protein was at least 95% pure as determined by Coomassie-stained SDS−PAGE gels (Figure 1) and was free from detectable topoisomerase and endo- and exonuclease activities. The concentration of RuvB protein was determined by the absorbance at 280 nm, using an extinction coefficient of $\epsilon_{280,native} = 1.64 \times 10^4\ M^{-1}\ cm^{-1}$ (Marrione & Cox, 1995). In side-by-side measurements of the concentration of RuvB protein preparations using either UV absorbance in concert with this extinction coefficient or Bradford assays with a BSA standard, the Bradford assay was found to overestimate the concentration of RuvB protein by a factor of 2.0. This has a substantial effect on comparisons between RuvA/RuvB stoichiometries reported under Results and those reported in the literature based on Bradford determinations of protein concentrations (Mitchell & West, 1994).

FIGURE 1: SDS−PAGE of purified RuvA and RuvB proteins. The molecular masses of the RuvA and RuvB proteins are 22.2 and 37.2 kDa, respectively. The RuvA and RuvB proteins migrate at 27 and 41 kDa, respectively. Lanes 1 and 4, BioRad low-range molecular mass markers; lane 2, RuvA protein; lane 3, RuvB protein. Both lanes 2 and 3 contain 15 μg of protein, as determined by UV absorption using their respective derived extinction coefficients. Note the heavier binding of Coomassie stain to the RuvB protein, an effect that leads to an overestimation of RuvB concentrations when the Bradford protein assay is used (see Materials and Methods).

Purification of the RuvA Protein. An 8-L culture of *E. coli* cells overexpressing the RuvA protein was grown overnight in 2 × YT media, pelleted, and lysed as described previously (Tsaneva et al., 1992a; Iype et al., 1994). All subsequent steps were carried out at 4 °C. Ammonium sulfate was added to the high-speed supernatant to 50% saturation. The precipitated proteins were pelleted at 13 000 rpm in a Beckman JA14 rotor. The RuvA protein was not precipitated. Solid ammonium sulfate was added to the supernatant to 70% saturation. The precipitated proteins, including RuvA protein, were pelleted as above. The pellet was dissolved in P100 buffer and dialyzed against the same buffer. The dialyzed protein solution was loaded onto a 50 mL (1.25 cm × 10 cm) Macroprep ceramic hydroxyapatite equilibrated in P100 buffer. The column was washed with 2 column volumes of P100 buffer and developed with a 500 mL linear gradient from 150 to 1000 mM KCl in P100 buffer. The RuvA protein peak (380−530 mM KCl) was dialyzed against P100 buffer and loaded onto the same hydroxyapatite column [after washing the column with 1 M potassium phosphate (pH 6.8) and reequilibrating with P100 buffer]. The column was washed with 2 column volumes of P100 buffer and developed with a 500 mL linear gradient from P100 to P600 buffer. RuvA protein peak fractions (250−340 mM potassium phosphate) were pooled, dialyzed extensively into RuvA storage buffer, and stored at −70 °C. The final yield of RuvA protein from 40 g wet weight of cells was 200 mg.

[1] Abbreviations: ssDNA, single-stranded DNA; dsDNA, double-stranded DNA; SDS−PAGE, sodium dodecyl sulfate−polyacrylamide gel electrophoresis; DTT, dithiothreitol; EDTA, ethylenediaminetetraacetic acid, SDS, sodium dodecyl sulfate; bp, base pair(s); kbp, kilobase pair(s); TLC, thin-layer chromatography.

The RuvA protein was greater than 95% pure as determined by Coomassie-stained SDS−PAGE gels (Figure 1) and was free from detectable topoisomerase, ATPase, and endo- or exonuclease activities (data not shown). The concentration of RuvA protein was determined using an extinction coefficient obtained using a method described elsewhere (Marrione & Cox, 1995). Six independent measurements on two different preparations of RuvA protein yielded an extinction coefficient of $\epsilon_{280,\text{native}} = (5.55 \pm 0.03) \times 10^3\ M^{-1}\ cm^{-1}$. The one cysteine residue present in RuvA monomers was ignored in the extinction coefficient determination. The absorbance maximum for the native and denatured protein is 280 nm. The A_{280}/A_{260} ratio for the native RuvA protein is 1.29 ± 0.01. In side-by-side measurements of the concentration of RuvA protein preparations using either UV absorbance in concert with this extinction coefficient or Bradford assays with a BSA standard, the two methods were found to give essentially identical results.

DNA Substrates. Circular single-stranded DNA from bacteriophage M13mp8 and supercoiled circular duplex pJFS35r DNAs were prepared using methods described previously (Davis et al., 1980; Messing, 1983; Neuendorf & Cox, 1986). The pJFS35r plasmid was over 95% supercoiled as determined by densitometric scanning of agarose gels (data not shown). The plasmid pJFS35r is a 2820 base pair plasmid derived from the plasmid pXF3, containing a copy of the recombination target site recognized by the yeast FLP recombinase inserted between the *Eco*RI and *Bam*HI sites (Senecoff & Cox, 1986). The concentrations of ssDNA and dsDNA were determined by the absorbance at 260 nm, using 36 and 50 $\mu g\ mL^{-1}\ A_{260}^{-1}$, respectively, as the conversion factors. DNA concentrations are reported in terms of total nucleotides.

Full-length linear duplex DNA was obtained by digesting the plasmid pJFS35r with the restriction endonuclease *Pst*I. Relaxed pJFS35r plasmid DNA was prepared from the supercoiled circular duplex plasmid pJFS35r by incubation with topoisomerase I. All restriction enzyme digestions were performed as recommended by the enzyme supplier. To purify DNAs following enzyme treatments, reaction mixtures were extracted sequentially with phenol/chloroform/isoamyl alcohol (25:24:1) and chloroform/isoamyl alcohol (24:1), followed by ethanol precipitation.

Assays To Measure ATP Hydrolysis. The coupled spectrophotometric assay used to measure ATP hydrolysis, employing pyruvate kinase and lactate dehydrogenase, and the alternative thin-layer chromatography procedure were both described previously (Morrical et al., 1986; Marrione & Cox, 1995). Kinetic effects described in the text affected the useful time period over which data could be collected in some experiments. In reactions with RuvA and RuvB proteins, no DNA, and 30 μM or less ATP, initial rates were derived from data collected in the first 5 min of the reaction (at later times, the rates were attenuated as described under Results).

Reactions were carried out at 37 °C in buffer A containing 3 mM NADH, an ATP regeneration system (20 units mL^{-1} pyruvate kinase and 7.5 mM PEP), and 20 units mL^{-1} lactate dehydrogenase, in a reaction volume of 400 μL. Reactions were preincubated for 10 min at 37 °C with all components except RuvA and RuvB, and initiated by the addition of a mixture of RuvA and RuvB proteins. All reactions were carried out with 1.0 μM RuvB and 1.3 μM RuvA proteins unless noted, and various types of DNA were included in some reactions as indicated in the figure legends and under Results. After addition of all reaction components, the final pH of the reaction mixtures is 7.7 at room temperature. For reactions with RuvB protein alone, conditions for ATP hydrolysis reactions were as described (Marrione & Cox, 1995). In a buffer essentially equivalent to buffer A with 1 mM ATP, Mitchell and West (1994) have reported that RuvB protein is in a hexameric form. We assume that a hexameric species is the predominant form of RuvB protein in all reactions.

In all experiments, ATP was added as an equimolar mixture of ATP and magnesium acetate to bring the ATP concentration to the indicated level (1 mM unless noted), generating a corresponding increase in the total Mg ion concentration. The concentration of free Mg ion was calculated by assuming a K_D' of 1.184×10^{-5} M for the MgATP complex under our typical reaction conditions of pH 7.7 and 37 °C, determined by published methods (O'Sullivan & Smithers, 1979). Where ATP concentrations or additions are reported in the text, the presence of an equimolar addition of Mg^{2+} is implied.

In some assays, the effect of adding circular single-stranded DNA, supercoiled DNA, or additional ATP to an ongoing ATPase assay was investigated. In experiments where DNA or ATP was added, reactions (400 μL) containing 15 μM ATP were initiated by the addition of a mixture of RuvA and RuvB proteins. These reactions were monitored for 10 min. At 10 min, the concentration of ATP in one reaction was increased to 1 mM by the addition of 20 μL of a prewarmed concentrated ATP stock solution in buffer A [or, alternatively, 20 μL of circular single-strand M13mp8 DNA or supercoiled pJFS35r plasmid DNA stock solution (in buffer A + 15 μM ATP) was added to give a final concentration of 100 μM nucleotides]. The control reactions received a 20 μL aliquot of 15 μM ATP in buffer A. After the addition, the reactions were monitored for an additional 20−30 min. The dilution effect from the 5% increase in solution volume had no significant effect on RuvB protein ATPase activity (data not shown). The dilution of RuvB protein after the addition was taken into account in calculating reaction rates.

For reactions with RuvB protein alone where RuvA protein was added, reactions (400 μL) containing 100 μM ATP were initiated by the addition of RuvB protein. These reactions were monitored for 30 min. At 30 min, the concentration of RuvA protein in one reaction was increased to 1.3 μM by the addition of 20 μL of a prewarmed concentrated RuvA stock solution in buffer A + 100 μM ATP. The control reaction received a 20 μL aliquot of buffer A + 100 μM ATP. The modest dilution factor was taken into account in the calculation of reaction rates as described above.

Burst kinetics in RuvB protein-mediated ATP hydrolysis reactions with RuvA protein were monitored by thin-layer chromatography. Reaction conditions are described in the figure legends and under Results. Reactions were preincubated for 10 min at 37 °C, and a mixture of RuvAB proteins was added and mixed thoroughly to initiate the reaction. The total reaction volume was 100 μL, and immediately after mixing, aliquots (1 μL) were removed and spotted onto TLC plates every 5 s up to 50 s, then every 10 s to 1.5 min, then every 15 s for the next minute, and then every 30 s during

the next 2.5 min (5 min or 23 aliquots total). Calculation of burst size is as previously described (Marrione & Cox, 1995). The results are the mean of four experiments at two different protein concentrations. The ratio of RuvB to RuvA protein monomers was kept constant at 6:8. The error is reported as the standard error of the mean.

Kinetic Data Analysis. Initial velocities of reactions (v_0) were analyzed using the program HYPER (Cleland, 1979a). This program fits initial reaction velocities to the Michaelis−Menten equation: $v_0 = k_{cat}[S]/(K_m + [S])$ by the least-squares method for the reciprocal plots. Repetitions of experiments were analyzed independently, and the results were averaged.

RESULTS

Experimental Design. Experiments were carried out to determine the effects of RuvA protein on all aspects of RuvB protein-mediated ATP hydrolysis. The work is divided into two parts. The first is a general characterization of the ATP hydrolytic reaction. The second part is a more directed study of a time-dependent attenuation of ATP hydrolysis observed under some conditions. Unless noted, all protein concentrations are reported in terms of monomers. Previous experiments showed that RuvB protein alone exhibited optimal ATP turnover at a concentration of approximately 1 μM RuvB monomers (Marrione & Cox, 1995), and this concentration of RuvB provided a starting point for the experiments below.

(I) Kinetics of RuvB-Mediated ATP Hydrolysis in the Presence of RuvA Protein

Effects of RuvA Protein on RuvB Protein-Mediated ATP Hydrolysis in the Absence of DNA. A number of experiments were carried out to define standard reaction conditions. In the presence of 1.3 μM RuvA protein, the RuvB protein-mediated ATPase activity exhibits Michaelis−Menten kinetics over the concentration range examined (10 μM to 3 mM) (Figure 2). These data provide a K_m value for ATP of 19.7 ± 2.0 μM ATP and a k_{cat} of 10.6 ± 0.2 min^{-1} (Table 1).

The effect of free magnesium ion concentration (magnesium in excess of that required to form a MgATP complex) on the RuvB protein ATPase activity in the presence of RuvA and 1 mM ATP is shown in Figure 3. Three different RuvA protein concentrations were examined with 1.0 μM RuvB protein. In each case, the ATPase activity of RuvB protein reaches a maximum at 10 mM free magnesium ion concentration. At a magnesium ion concentration equal to the ATP concentration (leaving approximately 0.1 mM free Mg^{2+}), the observed rates of ATP hydrolysis are 30%, 25%, and 20% the maximal rates observed with 0.67 μM, 1.0 μM, and 2.0 μM RuvA protein, respectively. A free magnesium ion concentration of approximately 10 mM (e.g., 11 mM total when 1 mM ATP is present) was adopted as standard and used in all further experiments with the RuvA and RuvB proteins.

The effect of varying the concentration of one protein at a fixed concentration of the other protein on rates of ATP hydrolysis is shown in Figure 4 and Table 1. In Figure 4A,B, the concentration of RuvA protein is held at 1.3 μM, and RuvB protein is varied from 0 to 10 μM. These data show that an apparent critical concentration of RuvB protein monomers, nearly 200 nM, must be exceeded before the RuvB protein complex can hydrolyze ATP. At 250 nM RuvB monomers, ATPase activity was detected with an apparent turnover number of 6.8 min^{-1}. The initial rate of ATP hydrolysis exhibits an approximately linear dependence on RuvB protein concentration from 500 nM to 2.0 μM RuvB protomers. In this range, the turnover number for ATP is 8.9 min^{-1}. Above 2 μM RuvB protein, the rate of ATP hydrolysis increases more slowly, and the apparent k_{cat} declines. A similar titration curve for RuvB protein is seen in the absence of RuvA protein, although rates are lower (Marrione & Cox, 1995). With or without RuvA protein, optimal ATP hydrolytic turnover is seen at a concentration of 1.0 μM RuvB protein monomers, in the linear region of the protein titration curve, and this concentration is retained as standard in the remaining experiments except as noted.

The effect of varying RuvA protein concentration on RuvB protein-mediated ATP hydrolysis in the presence or absence of DNA is shown in Figure 4C−E and Table 1. In reactions without DNA (Figure 4C), RuvA protein concentration was varied at three different RuvB protein concentrations. The

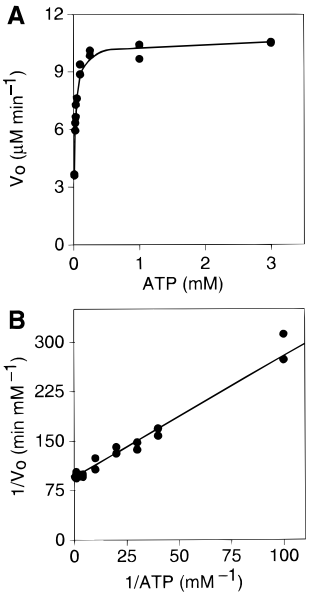

FIGURE 2: Steady-state kinetic analysis of RuvB protein-mediated ATP hydrolysis with RuvA protein in the absence of DNA. Reactions were carried out as described under Materials and Methods. Assays contained 1.0 μM RuvB protein monomers and 1.3 μM RuvA protein monomers and covered a range of substrate ATP concentrations from 10 μM to 3 mM. Each point represents an individual experiment, with duplicate experiments (same ATP concentration) always done on different days. Lines represent the fitted data analysis by HYPER.

Table 1: Summary of Derived Steady-State Rate Constants for RuvB Protein-Mediated ATP Hydrolysis with Varying Concentrations of RuvA Protein at a Constant RuvB Protein Concentration of 1.0 μM[a]

[RuvA] (μM)	[RuvB] (μM)	RuvA:RuvB monomer ratio	derived K_m (μM ATP)	derived k_{cat} (min^{-1})
0	1.0	0:6	147 ± 29	4.81 ± 0.21
0.33	1.0	2:6	12.6 ± 1.2	6.92 ± 0.12
0.67	1.0	4:6	17.4 ± 1.4	8.95 ± 0.13
1.3	1.0	8:6	19.7 ± 2.0	10.6 ± 0.24
2.0	1.0	12:6	13.9 ± 2.3	11.0 ± 0.28

[a] All reactions contained 1.0 μM RuvB protein, no DNA, and the corresponding concentrations of RuvA protein. Procedures and program used in the data analysis are described under Materials and Methods. Reactions with no RuvA and 1.3 μM RuvA protein are in duplicate, and the other values are derived from experiments performed once.

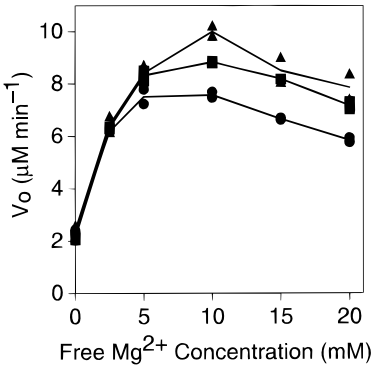

FIGURE 3: Effects of free [Mg^{2+}] on RuvB protein-mediated ATP hydrolysis with RuvA in the absence of DNA. All rates were obtained as described under Materials and Methods. All reactions contained 1.0 μM RuvB protein, 1 mM ATP, and 0.67 μM (●), 1.0 μM (■), or 2.0 μM (▲) RuvA protein. Two separate experiments are shown at each Mg^{2+} concentration. Rates are plotted against an assumed free Mg^{2+} concentration, calculated as described under Materials and Methods. The lowest total Mg^{2+} concentration used, 1 mM, gives a calculated free Mg^{2+} concentration of 0.103 mM. At higher concentrations of Mg^{2+}, the concentration of free Mg ion is essentially equivalent to that in excess of the ATP concentration. For example, where the total Mg ion concentration is 3.5 mM, the calculated concentration of free Mg^{2+} is 2.508 mM.

ATP hydrolysis rates reach a maximum at 0.67, 1.33, and 2.67 μM RuvA protein at 0.5, 1.0, and 2.0 μM RuvB protein, respectively. At a protein monomer to monomer ratio, ATPase rates peak at 6 RuvB protein monomers to 8 RuvA protein monomers in each case.

To further define the optimal RuvB to RuvA protein ratio, a steady-state kinetic analysis of ATP hydrolysis was performed at different RuvA concentrations, each at 1.0 μM RuvB (Table 1). When RuvA protein is not present in the reaction mixture, the K_m and k_{cat} values are 147 $\pm$ 29 μM and 4.81 $\pm$ 0.21 min^{-1}, respectively, in good agreement with previous data (Marrione & Cox, 1995). As RuvA protein concentration increases from 0.33 to 2.0 μM monomers, the K_m values for the RuvB ATPase activity remain constant (within experimental error) at about 15 μM ATP, but the turnover number increases until a maximum is reached at 1.3 μM RuvA. It then levels off within experimental error at approximately 11 min^{-1}. These data and those presented above indicate that a ratio of RuvB protein monomers to RuvA protein monomers of 6 to 8 is optimal for ATPase activity in the absence of DNA.

To determine if the optimal RuvA/RuvB ratio held when DNA is present in the reaction, RuvA protein concentration was varied at 1 μM RuvB protein with circular ssM13mp8 (Figure 4D) or supercoiled pJFS35r (Figure 4E). In both cases, the ATPase activity reached a maximum or leveled off at 1.3 μM RuvA protein. These data correspond to a ratio of 6 RuvB protein monomers to 8 RuvA protein monomers for optimal rates of ATP hydrolysis with or without DNA. A concentration of 1.3 μM RuvA protein was adopted as standard in the remaining experiments except as noted. In experiments where 1.0 μM RuvB and 1.3 μM RuvA proteins are combined, an abbreviated protein designation of RuvAB is used to reflect the presumed complex present as the active species.

Effects of ssDNA and Supercoiled DNA on RuvB Protein-Mediated ATP Hydrolysis with RuvA Protein. A steady-state kinetic analysis of RuvB protein-mediated ATP hydrolysis in the presence of RuvA protein was carried out with two different types of DNA, with results summarized

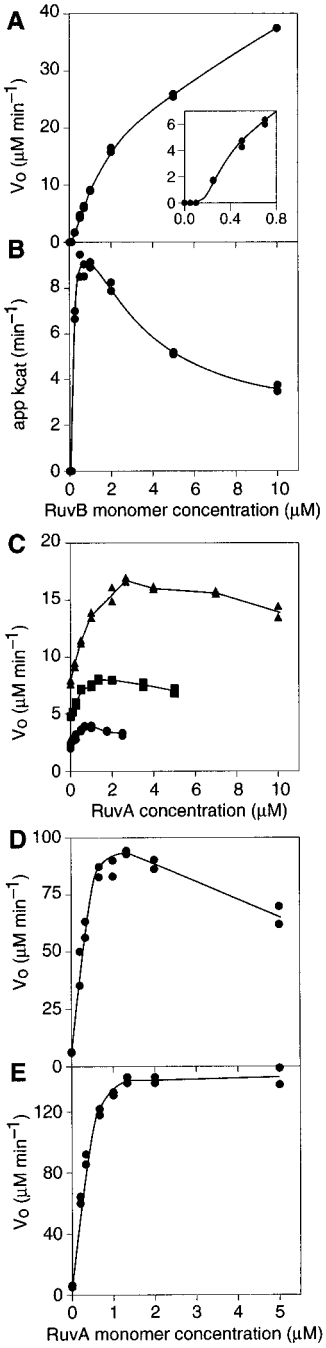

FIGURE 4: Dependence of RuvB protein-mediated ATP hydrolysis on RuvB and RuvA monomer concentrations, with and without DNA. All reactions were carried out as described under Materials and Methods, and contained 1 mM ATP. For measurements with low concentrations of RuvA or RuvB protein, the protein was diluted into RuvAB dilution buffer as required. In panels A and B, all reactions contained 1.3 μM RuvA protein and no DNA, and RuvB protein concentrations were varied as shown. Initial rates are plotted in panel A, with data obtained at low RuvB protein concentrations expanded in the inset. In panel B, the data in panel A are divided by the concentration of RuvB protein to yield apparent k_{cat} values. In panels C−E, the RuvA protein concentration is varied while the RuvB concentration is held constant. Initial rates are plotted in each panel. In panel C, reactions contained no DNA and 0.5 μM (●), 1.0 μM (■), or 2.0 μM (▲) RuvB protein. In panel D, reactions contained 100 μM circular single-stranded M13mp8 DNA and 1.0 μM RuvB protein. In panel E, reactions contained 100 μM supercoiled pJFS35r DNA and 1.0 μM RuvB protein.

Table 2: Summary of Derived Steady-State Kinetic Constants for RuvAB Protein-Mediated ATP Hydrolysis[a]

DNA	derived K_m (μM ATP)	derived k_{cat} (min^{-1})
none	19.7 ± 2.0	10.6 ± 0.24
circular ssDNA	71.5 ± 8.8	112 ± 7
supercoiled DNA	17.0 ± 1.6	143 ± 3
linear dsDNA	SI	SI

[a] All reactions contained 1.0 μM RuvB protein and 1.3 μM RuvA protein. Procedures and program for data analysis are described under Materials and Methods. All DNA concentrations are 100 μM. The ssDNA substrate is M13mp8, and dsDNA substrates are derived from the plasmid pJFS35r as described under Materials and Methods. SI means partial substrate inhibition. Data are derived by averaging at least 2 experiments performed on different days.

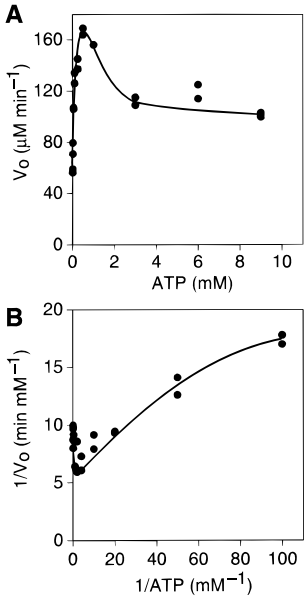

FIGURE 5: Steady-state kinetic analysis of RuvB protein-mediated ATP hydrolysis in the presence of RuvA protein and linear dsDNA. Reactions were carried out as described under Materials and Methods, and contained 1.0 μM RuvB protein, 1.3 μM RuvA protein, and 100 μM linear double-strand pJFS35r plasmid DNA. Substrate ATP concentrations ranged from 10 μM to 9 mM. Two separate experiments are shown at each ATP concentration. Lines drawn through the data are approximate and are not fitted to any data analysis program.

in Table 2. The RuvB protein ATPase activity again obeys Michaelis−Menten kinetics in the examined range of ATP concentrations from 10 μM to 3 mM (data not shown). For reactions with 100 μM M13mp8 ssDNA, these data provide a K_m of 71.5 ± 8.8 μM ATP and a k_{cat} of 112 ± 7 min^{-1}. For reactions with 100 μM pJFS35r supercoiled DNA, the K_m is 17.0 ± 1.6 μM ATP, and the k_{cat} is 143 ± 3 min^{-1}. No lag in ATP hydrolysis rates was observed when both RuvA and RuvB proteins were present in the reaction mixture with ssDNA or supercoiled DNA at 37 °C (data not shown). Both DNAs greatly stimulate the rates of ATP hydrolysis, but they have very different effects on the K_m. The stimulation of ATP hydrolysis by both ssDNA and supercoiled dsDNA is much greater than that seen in the absence of RuvA protein (Marrione & Cox, 1995).

Effect of Linear Double-Stranded pJFS35r DNA on RuvAB Protein-Mediated ATP Hydrolysis. Results obtained with linear duplex DNA were dramatically different. Figure 5 illustrates the effect of linear double-stranded DNA on the RuvAB complex ATPase activity. As the ATP concentration

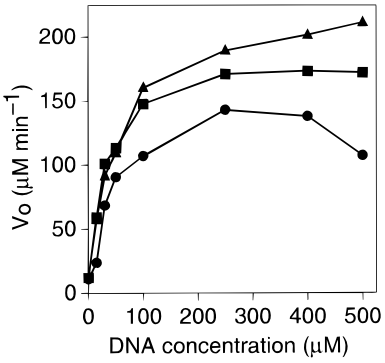

FIGURE 6: Effect of DNA concentration on the rate of RuvB-mediated ATP hydrolysis in the presence of RuvA protein. All reactions contained 1.0 μM RuvB protein, 1.3 μM RuvA protein, 1 mM ATP, and 100 μM of the indicated DNA, and are carried out as described under Materials and Methods. The effects of ssDNA (●), supercoiled dsDNA (■), or closed circular dsDNA relaxed with topoisomerase I (▲) are shown.

increases from 10 to 500 μM, there is an increase in ATP hydrolysis rates peaking at an initial rate of over 160 μM ATP min^{-1}. However, as the ATP concentration increases further from 1 to 3 mM, the initial rates of ATP hydrolysis decrease. The rates level off at the highest ATP concentrations (6 and 9 mM ATP), reflecting a partial substrate inhibition. Due to the complexities involved in analyzing partial substrate inhibition, no effort was made to derive extrapolated steady-state kinetic data. However, the maximal level of ATPase activity is comparable to that measured with supercoiled DNA in the reaction. This effect showed no dependence on the identity of the plasmid used to generate the linear dsDNA, on DNA length, or on a particular protein preparation (data not shown). Substrate inhibition was not observed in RuvAB reactions when relaxed, circular pJFS345r DNA was used as a DNA cofactor (data not shown), so DNA linearity appears to be required.

Effect of DNA Concentration on RuvAB Complex ATPase Activity. The effect of the concentration of various DNAs on ATP hydrolysis at a constant ATP concentration is shown in Figure 6. A dramatic increase in ATP hydrolysis rates is observed for reactions with any type of DNA (M13mp8 ssDNA, or pJFS35r dsDNA either supercoiled or relaxed with topoisomerase I). For reactions with ssDNA, the rates appear to level off around 250 μM nucleotides and then start to decrease at higher DNA concentrations. The patterns are similar for the dsDNAs except the rates of ATP hydrolysis do not decrease at high DNA concentrations. Rates exhibit a continuing slow increase with topoisomerase I relaxed pJFS35r DNA even at the higher concentrations examined. At the highest concentration of topoisomerase I relaxed pJFS35r (500 μM), the actual concentration of DNA molecules is 88.7 nM. The concentration of RuvB hexamers (assuming all of the RuvB is in the hexameric form) is 167 nM. This corresponds to 2 RuvB hexamers and 16 RuvA monomers per molecule of relaxed circular pJFS35r DNA.

A Burst in RuvAB Complex-Mediated ATP Hydrolysis. To examine a single turnover in the ATP hydrolytic reaction, the RuvB protein concentration was increased and the RuvA protein concentration was increased accordingly to keep the ratio of RuvB protomers to RuvA protein monomers at 6 to 8. In Figure 7, a burst is seen with no DNA or ssDNA present in the reaction mixture. In both sets of reactions, RuvB protein concentration was either 5.0 or 10.0 μM in

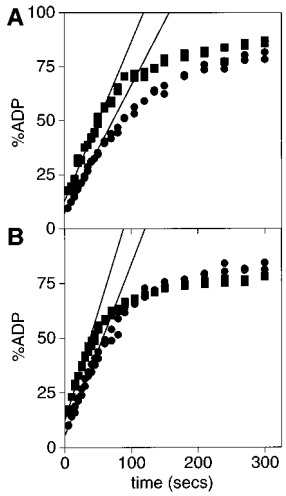

FIGURE 7: Burst in ATP hydrolysis. Reactions were carried out with the TLC assay as described under Materials and Methods. All reactions contained 25 μM ATP, and either 5 μM RuvB protein with 6.6 μM RuvA protein (●) or 10 μM RuvB protein with 13.3 μM RuvA protein (■). Panel A, reactions contained no DNA. Panel B, reactions contained 100 μM ssDNA.

Table 3: Summary of Burst Kinetics for RuvB Protein-Mediated ATP Hydrolysis[a]

DNA	[RuvB] (μM)	[RuvA] (μM)	burst size (μM ATP)	RuvB:ATP ratio monomer:molecule
none	5	6.67	1.66	3.01:1
	5	6.67	1.63	3.06:1
	10	13.3	3.16	3.16:1
	10	13.3	3.35	2.99:1
circular ssDNA	5	6.67	1.60	3.10:1
	5	6.67	1.63	3.06:1
	10	13.3	3.40	2.90:1
	10	13.3	3.39	2.95:1

[a] Reactions contained 25 μM ATP, and either 5 μM RuvB or 10 μM RuvB and the corresponding amount of RuvA protein to keep the ratio of RuvB monomers to RuvA monomers at 6 to 8. Procedures and calculation of bursts were done as described. The ssDNA substrate is M13mp8. Each reported burst is derived from a single experiment.

monomers. Lines fitted to these data and extrapolated to zero time give a burst of 1 ATP per 3.1 (±0.1) and 3.0 (±0.1) RuvB monomers in experiments with no DNA or ssDNA, respectively (Table 3). The calculated burst size represents the mean of 4 determinations, with the error reported as the standard error of the mean. These data are consistent with a burst of ATP hydrolysis corresponding to 2 ATPs per RuvB protein hexamer, and are in agreement with a previous report (Marrione & Cox, 1995). Due to technical limitations of the assay, higher protein concentrations and the effects of supercoiled DNA could not be examined.

(II) Attenuation of ATP Hydrolysis

Slow Inactivation of RuvB Protein-Mediated ATP Hydrolysis at ATP Concentrations Below the K_m. The coupled spectrophotometric ATPase assay includes an ATP regeneration system, maintaining the concentration of ATP at the initial concentration throughout the assay. As a result, no ADP accumulates during the reaction, and RuvB protein should hydrolyze ATP at a constant rate.

In the absence of RuvA protein, a reversible attenuation of RuvB protein-mediated ATP hydrolysis was previously observed at ATP concentrations near its K_m (Marrione & Cox, 1995). ATP hydrolysis simply stopped after about 60

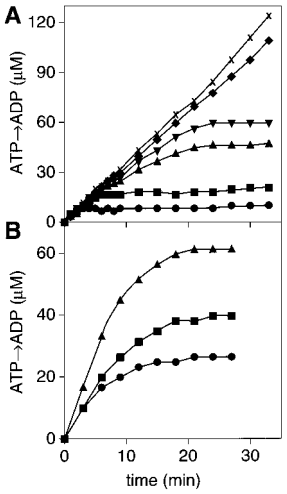

FIGURE 8: Attenuation of RuvB protein-mediated ATP hydrolysis. Reactions were carried out with the coupled spectrophotometric assay as described under Materials and Methods and contained no DNA. Panel A shows the time course of RuvB protein-mediated ATP hydrolysis in the presence of 50 μM (●), 75 μM (■), 100 μM (▲), 125 μM (▼), 200 μM (◆), and 250 μM (×) ATP. All reactions contained 1.0 μM RuvB protein. Panel B illustrates the effect of RuvB protein monomer concentration on the amount of ATP hydrolyzed before attenuation. Reactions contain 100 μM ATP and 0.5 μM (●), 1.0 μM (■), or 2.0 μM (▲) RuvB protein.

turnovers. The attenuation did not involve product inhibition or removal of ATP by contaminating processes (Marrione & Cox, 1995, and data not shown). Results presented in Figure 8 demonstrate that the effect is general for ATP concentrations at or below the K_m. For the RuvB protein alone, the K_m for ATP is 147 μM ATP (Table 1). At ATP concentrations from 50 to 125 μM, hydrolysis continues for a short time and then levels off. The degree of attenuation is a function of ATP concentration, with the length of time required before complete cessation of ATP hydrolysis is observed increasing with ATP concentration. At 50 μM ATP, only about 10 ATP hydrolytic turnovers per RuvB monomer are observed before cessation of ATP hydrolysis, compared to nearly 60 turnovers when ATP is present at 125 μM. Once the ATP concentration is above the K_m for ATP (data with 200 or 250 μM ATP in Figure 8), the RuvB protein hydrolyzes ATP at a constant rate and attenuation is not observed.

At a given ATP concentration, the number of turnovers per RuvB monomer prior to complete attenuation of ATP hydrolysis is independent of RuvB protein concentration. In panel B of Figure 8, the RuvB protein concentration is varied at a constant ATP concentration of 100 μM. As the RuvB protein concentration is increased from 0.5 to 2 μM, the total amount of ATP hydrolyzed prior to attenuation increases correspondingly. In all cases, about 30−40 ATPs are hydrolyzed per RuvB monomer.

The attenuation is readily reversible. Addition of ATP to concentrations above the K_m immediately restored the ATP hydrolytic activity to rates comparable to those observed when the higher ATP concentration was present at the beginning of the reaction (Marrione & Cox, 1995, and data not shown). The attenuation is not reversed by DNA, however. With RuvB protein alone, attenuation is observed even in the presence of ssDNA or linear dsDNA. Attenuation does not occur with circular dsDNA present, but addition of circular dsDNA after attenuation has occurred

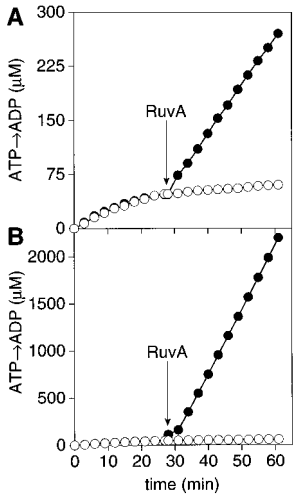

FIGURE 9: Effects of RuvA protein or DNA on the attenuation of RuvB protein-mediated ATP hydrolysis. Reactions were carried out with the coupled spectrophotometric assay as described under Materials and Methods. All reactions contained 1.0 μM RuvB protein and 100 μM ATP. Panels A and B contain no DNA and 100 μM ssDNA present from the beginning of the reaction, respectively. Individual reactions received RuvA protein (●) to a final concentration of 1.3 μM or an equal volume of RuvA protein storage buffer (○).

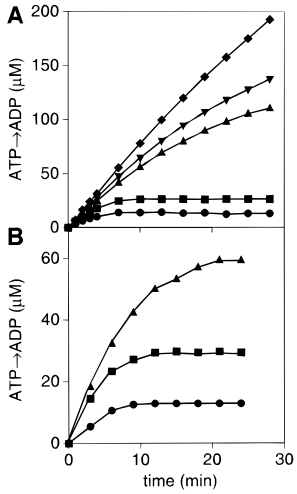

FIGURE 10: Attenuation of RuvB protein-mediated ATP hydrolysis when RuvA protein is present. Reactions were carried out with the coupled spectrophotometric assay as described under Materials and Methods. Panel A shows the time course of RuvB protein-mediated ATP hydrolysis with RuvA protein in the presence of 10 μM (●), 15 μM (■), 25 μM (▲), 33 μM (▼), and 50 μM (◆) ATP. All reactions have 1.0 μM RuvB protein and 1.3 μM RuvA protein. Panel B demonstrates the effect of RuvB protein monomer concentration on the amount of ATP hydrolyzed before attenuation when RuvA protein is present. All reactions contained 15 μM ATP, with 0.5 μM RuvB protein and 0.67 μM RuvA protein (●), 1.0 μM RuvB protein and 1.3 μM RuvA protein (■), or 2.0 μM RuvB protein and 2.7 μM RuvA protein (▲).

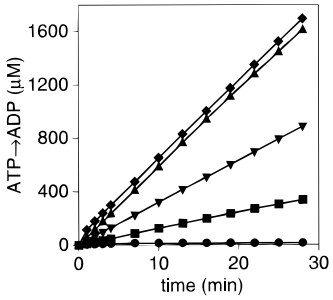

FIGURE 11: Lack of attenuation of RuvB protein-mediated ATP hydrolysis in the presence of RuvA protein and DNA. Reactions were carried out with the coupled spectrophotometric assay as described under Materials and Methods. All reactions contained 1.0 μM RuvB protein, 1.3 μM RuvA protein, and 100 μM of the indicated DNA. The lines show the effect of no DNA with 10 μM ATP (●), M13mp8 ssDNA with 10 μM ATP (■), supercoiled pJFS35r DNA and 5 μM (▼) and 10 μM (▲) ATP, or linear pJFS35r dsDNA with 10 μM ATP (◆).

does not restore the reaction (Marrione & Cox, 1995). In the present work, we confirmed that the addition of any form of DNA (circular ssDNA, linear dsDNA, or supercoiled DNA) does not lead to a restart of ATP hydrolysis or otherwise affect attenuated reactions (data not shown).

The addition of RuvA protein can relieve the attenuation observed with RuvB protein alone (Figure 9). Pairs of reactions were initiated with 1 μM RuvB protein and either no DNA (panel A) or 100 μM ssDNA (panel B). After attenuation had occurred, RuvA protein was added to one reaction in each pair to a concentration of 1.3 μM. This led to an immediate resumption of ATP hydrolysis with no evident lag. Final rates of ATP hydrolysis were comparable to reactions with RuvA protein present from the beginning (7 and 60 μM min^{-1} for reactions with no DNA and ssDNA, respectively).

As shown in Table 1, the presence of RuvA protein leads to a substantial decline in the K_m for ATP of the RuvB protein ATPase activity. Where 100 μM ATP is below the K_m observed with RuvB protein alone, it is much above the K_m for the RuvAB protein complexes. Therefore, the results in Figure 9 do not eliminate the possibility that a K_m-sensitive attenuation of ATP hydrolysis could occur in reactions containing both RuvA and RuvB proteins, where the K_m for ATP is decreased to 19.7 μM (Table 1). In Figure 10, we demonstrate that attenuation still occurs and still exhibits a dependence on the K_m for ATP. In panel A, attenuation is evident at 10 or 15 μM ATP, but becomes much less pronounced or absent at ATP concentrations of 25 μM and above. At 10 and 15 μM ATP, a definitive end point is reached after 5 min with approximately 15 and 25 ATPs hydrolyzed per RuvB monomer, respectively. At 25 and 33 μM ATP, total attenuation is not achieved, but the time course becomes nonlinear after 15 min. The progress of ATP hydrolysis is linear at 50 μM ATP.

In panel B of Figure 10, the RuvB and RuvA protein concentrations are varied at a constant ATP concentration of 15 μM. The ratio of RuvB monomers to RuvA monomers is maintained at 6 to 8. As with RuvB alone, the number of turnovers per RuvB monomer appears to be independent of RuvAB concentration. About 30 ATPs are hydrolyzed per RuvB monomer prior to cessation of the reaction, with the total ATP hydrolyzed depending only on the concentration of RuvB protein present.

DNA has a much greater effect on the attenuation process when RuvA protein is present than is observed in its absence. When RuvA protein is present, any form of DNA abolishes the attenuation. Figure 11 illustrates the effect of various DNAs on the time course of RuvB protein-mediated ATP hydrolysis when RuvA protein is present and substrate concentrations are below the K_m. All reactions contained 100 μM DNA (present from the beginning of the reaction) and either 5 or 10 μM ATP. The rate of ATP hydrolysis remained constant in each reaction containing DNA. For

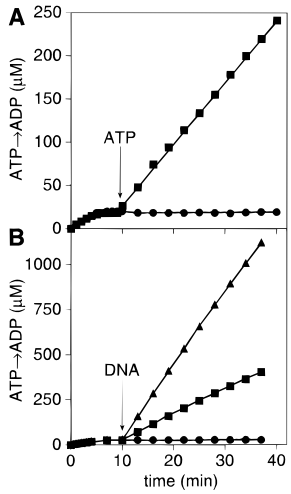

FIGURE 12: Effects of ATP or DNA on the attenuation of RuvB protein-mediated ATP hydrolysis in the presence of RuvA protein. Reactions were carried out with the coupled spectrophotometric assay as described under Materials and Methods, and contained 1.0 μM RuvB protein, 1.3 μM RuvA protein, and 15 μM ATP. In panel A, the individual reactions contained no addition (●) or addition of ATP to 1 mM (■). In panel B, the individual reactions received the indicated DNAs to 100 μM final concentration: no addition (●), M13mp8 ssDNA (■), or supercoiled pJFS35r DNA (▲).

reactions with ssDNA, no attenuation occurs even though the concentration of ATP is well below the K_m (71.5 μM; Table 2).

As was the case with RuvB protein alone (Marrione & Cox, 1995), the attenuation of ATP hydrolysis seen with the RuvAB complexes (without DNA) is immediately reversed simply by adding ATP to higher concentrations. In Figure 12, panel A, ATPase attenuation in the presence of 15 μM ATP is shown. Addition of ATP to a concentration of 1 mM results in an immediate resumption of ATP hydrolysis. The final rate of ATP hydrolysis (8 μM min^{-1}) is comparable to reactions that contained 1 mM ATP from the beginning.

Unlike the case with RuvB protein alone, attenuation in reactions with the RuvAB complexes can be reversed by the addition of DNA. In Figure 12, panel B, the addition of ssDNA or supercoiled DNA (triangles) to an attenuated reaction at 15 μM ATP results in an immediate resumption of ATP hydrolysis. The rates after resumption, 18 μM min^{-1} for ssDNA and 50 μM min^{-1} for supercoiled DNA, were comparable to reactions in which the DNA was present from the beginning.

DISCUSSION

We derive two major conclusions from this work. The first is that interaction with RuvA protein greatly affects the ATPase activity of the RuvB protein. This comes primarily from the steady-state kinetic analysis of ATP hydrolysis, and it complements and extends a number of previous observations (Tsaneva et al., 1992b; Mitchell & West, 1994). The complex formed with RuvA protein and RuvB protein leads to a 2−2.5-fold stimulation of ATP turnover in the absence of DNA. The K_m for ATP also declines 7−8-fold. Perhaps the major effect of RuvA protein is its enhancement of the effects of DNA on the RuvB protein ATPase. Where ssDNA or linear dsDNA has little effect on the ATPase activity of RuvB protein alone (Marrione & Cox, 1995), these DNAs increase the k_{cat} by an order of magnitude when RuvA is present. RuvA also eliminates a lag in reaching the maximum ATPase rate with circular dsDNA that is observed with RuvB alone. The results imply that RuvB is in much more intimate and continuous contact with DNAs of all forms when RuvA is present. They are also consistent with previous suggestions (Tsaneva et al., 1992b; West & Connolly, 1992; MItchell & West, 1994; Müller & West, 1994) that RuvA facilitates the loading of RuvB protein onto DNA.

All effects of RuvA protein are optimal at a RuvA/RuvB ratio of 8:6, suggesting the existence of a tight complex with this composition. This ratio is distinct from the 4:6 ratio reported previously (Mitchell & West, 1994). We believe the discrepancy is due to differences in the methods used to measure RuvB protein concentration, as described under Materials and Methods. We note that the stoichiometry may change when RuvAB is bound at a Holliday junction, where two RuvB hexamers appear to act with RuvA protein in promoting branch migration (Hiom & West, 1995; Parsons et al., 1995).

The stoichiometric requirement for RuvA protein in order to provide maximal enhancement of the ATPase activity of RuvB protein suggests that the two proteins interact in a direct and continuous fashion in these reactions. If RuvA protein instead functioned transiently for the loading of RuvB protein onto the DNA, RuvA protein might be required in only catalytic amounts. A direct interaction between the two proteins at Holliday junctions is evident in electron micrographs published recently by West, Stasiak, and their colleagues (Parsons et al., 1995). The RuvA and RuvB proteins also comigrate in experiments involving glycerol gradients, gel filtration, and gel-mobility shifts either without DNA or in the presence of dsDNA substrates (Iwasaki et al., 1992; Müller et al., 1993b; Shiba et al., 1993; Mitchell & West, 1994). The RuvA protein also enhances the gel-mobility shift conferred on ssDNA by RuvB protein (P. E. Marrione, unpublished results).

The second conclusion is that definable subsets (probably pairs) of the monomers that make up a RuvB hexamer are coordinated in their function, and that ligand binding in any subset of monomers has substantial allosteric effects throughout the hexamer. We frame this discussion in terms of coordinated pairs of monomers based on the results of the burst experiments. Two plausible schemes for subunit pairing are presented in Figure 13. In both cases, the series of steps in the ATP hydrolytic cycle are the same. At any given moment, one pair of monomers is in a conformation to which ATP binds very tightly (pair A). The ATP is rapidly hydrolyzed to generate bound ADP and P_i. The turnover of the complex with ADP and P_i is rate-limiting in the overall ATP hydrolytic pathway. Turnover is facilitated by the binding of ATP to a second pair of monomers in the hexamer (pair B). In this way, ATP not only is a substrate for hydrolysis by monomer pair B but also is a homotropic allosteric effector of a key step in the ATP hydrolytic cycle in monomer pair A. Although other aspects of the cycle are more speculative, it is logical to postulate that ATP would subsequently be hydrolyzed by pair B, with turnover facilitated by ATP binding to pair C. Each pair of monomers would move cyclically through a set of at least three conformations, with each conformational change modulated by interactions with the other monomers. The measured K_m for ATP hydrolysis reflects the initial (allosteric) interaction

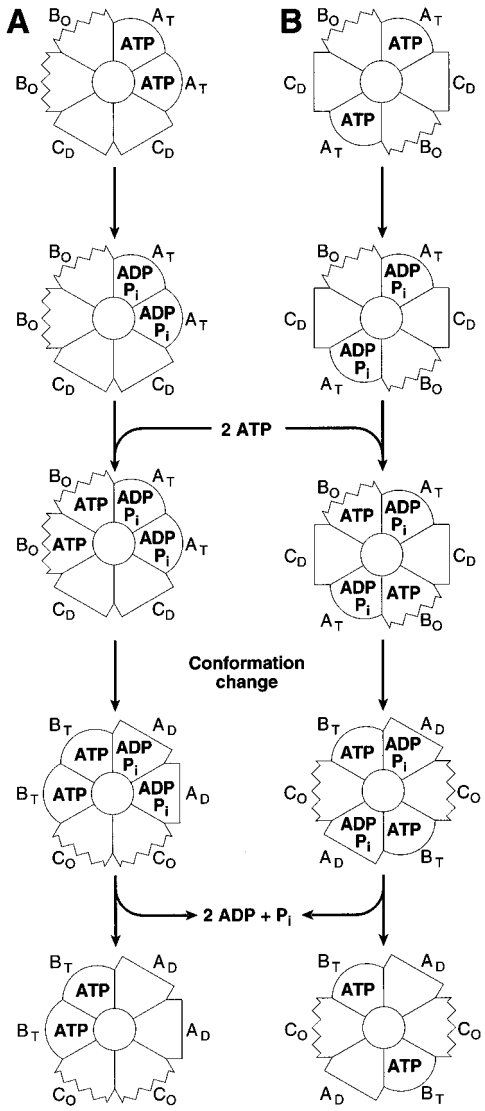

FIGURE 13: Models. A plausible sequence of steps in the ATP hydrolytic pathway of RuvB protein is depicted. The activities of pairs of subunits within the RuvB hexamer are coordinated. Pathways A and B illustrate two possibilities for subunit pairing. The paired subunits are denoted A, B, and C. The letters subscripted, T, D, and O, denote distinct conformational states through which each subunit pair cycles. Scheme A is similar to a pathway proposed for the mitochondrial F_1-ATPase (Abrahams et al., 1994).

of ATP with pair B, and the similar interaction of ATP with each successive pair of monomers.

The results of this study provide evidence supporting several aspects of the proposed hydrolytic cycle. The burst kinetics support the idea of an asymmetric RuvB hexamer containing functionally paired monomers, and indicate that a subset of RuvB monomers bind to ATP very tightly. A burst phase in which 2 ATPs per hexamer are hydrolyzed is observed with RuvB alone (Marrione & Cox, 1995), and results reported here show that an identical burst is observed in the presence of RuvA protein. For RuvB alone, the size of the burst exhibits no dependence on ATP concentration even though the concentrations used to observe it are below the K_m (Marrione & Cox, 1995). This indicates that the first ATPs bound and hydrolyzed are bound with an affinity much greater than that reflected in the K_m.

The attenuation effect provides evidence that binding of ATP to a second subset of RuvB monomers facilitates turnover in the first. In contrast to the burst kinetics, attenuation is very sensitive to the K_m for ATP. Below the K_m, the attenuation occurs more rapidly as ATP concentrations decrease. Above the K_m, attenuation does not occur. This can be interpreted in terms of the proposed allosteric effects of ATP. Below the K_m, there is insufficient ATP to saturate the binding sites involved in the allosteric effect. One possibility is that the binding of one ATP instead of two to a second monomer pair (monomer pair B, for example) leads to an attenuated complex in which turnover in another monomer pair (e.g., A) has been blocked. The probability of this happening would increase as ATP concentration declined below the K_m, leading to the observed decrease in the number of turnovers observed prior to attenuation at lower ATP concentrations. ATP turnover in the attenuated complexes is immediately restored upon addition of ATP to concentrations above the K_m. This is true whether RuvA protein is present or not. The major distinction is that DNA also rescues the attenuated complexes or prevents its occurrence only when RuvA protein is present, again reflecting the more intimate association with DNA brought about by RuvA. If the reversal of attenuation involves a change in conformation in some part of the RuvB hexamer, then both DNA and the RuvA protein itself may be considered allosteric effectors of RuvB-mediated ATP hydrolysis.

When DNA is present, the conformation changes must be coupled to transient interactions with the DNA leading to translocation on and limited unwinding of the DNA. For example, one of the proposed conformations might bind tightly to single-stranded DNA as an intermediate in the helicase activity of the RuvAB complex. A better description of how the proposed ATP hydrolytic cycle (Figure 13) might be coupled to DNA unwinding and movement of the complex on the DNA must await more detailed information of the DNA binding properties of RuvAB. With complexes of RuvA and RuvB bound at the branched DNA intermediates of recombinational DNA repair, the ATP hydrolysis would be coupled to movement of the DNA branch as proposed by West and colleagues (Parsons et al., 1995).

The existence of nonequivalent active sites in multisubunit enzymes that hydrolyze or synthesize ATP appears to be a general theme. Several other hexameric helicases have been shown to possess tight and weak binding sites for ATP (Geiselmann & von Hippel, 1992; Bujalowski & Klonowska, 1993; Dong et al., 1995; Patel & Hingorani, 1995), although there are often three rather than two high-affinity sites. The theme is by no means limited to helicases. One of the schemes in Figure 13 is very similar (in reverse) to a pathway proposed for ATP synthesis by the mitochondrial F1-ATPase (Abrahams et al., 1994; Pedersen, 1994).

Substrate inhibition by high concentrations of ATP of the RuvB protein ATPase activity has been reported previously (Marrione & Cox, 1995), but this represents another property that is altered by the RuvA protein. With RuvB protein alone, closed circular dsDNA stimulates ATP hydrolysis greatly, and ATP substrate inhibition is observed. Linear dsDNA produces only a modest stimulation of the ATPase activity, and the substrate inhibition is not observed (Marrione & Cox, 1995). When RuvA protein is present, the pattern changes. Both linear and circular dsDNA molecules produce large stimulations in ATPase activity. However, substrate inhibition is observed in the presence of linear

dsDNA but not with supercoiled DNA. A reason for this difference cannot not be provided at this time, but the substrate inhibition is still potentially informative. For single substrate enzymes (such as NTPases), a limited number of reasons can account for the partial substrate inhibition (Cleland, 1979). Two subsrate molecules may bind unproductively in the active site and cause the inhibition. Second, an alternative reaction pathway may be occurring at the high substrate concentrations. Third, nonspecific inhibition may result due to ionic strength or toxic counterions from the substrate. Finally, higher substrate concentrations may allow substrate binding to alternative ATP binding sites of lower affinity in the RuvB hexamer. The first three possibilities are improbable because they usually obtain only at very high substrate concentrations (greater than 10−20 mM). The inhibition seen in these studies is evident with as little as 1 mM ATP, where substrate inhibition is unusual (Cleland, 1979). Sufficient evidence exists for substrate binding sites in the RuvB protein hexamer with different affinities for ATP substrate. Therefore, the presence of binding sites with different affinities for substrate seems at least a plausible explanation for the substrate inhibition. In the paired RuvB monomers scenario outlined above, for example, premature binding of ATP to monomer pair C might cause the inhibition. With RuvA protein in the reaction mixture, we have observed the effect only with linear dsDNA. This suggests that the substrate inhibition occurs in complexes stalled when they reach a DNA end. For example, unproductive binding of ATP to the "wrong" RuvB monomer pairs (whichever monomers have ATP sites with lower affinities at any particular moment) might inhibit the dissociation of RuvAB complexes when they encounter a DNA end and/or rebinding to new DNAs. Since the length of the DNA does not seem to affect the kinetics, we presume that any movement along the DNA is fast and not rate-limiting.

Overall, the data are consistent with the concept of a RuvAB complex in tight association with the DNA, translocating on the DNA in a reaction coupled to ATP hydrolysis. When bound at a DNA branch, the translocation process brings about branch migration as part of a larger pathway for processing recombination intermediates created by the action of RecA protein (Shinagawa et al., 1991; West & Connolly, 1992; Kuzminov, 1993; West et al., 1993; Müller & West, 1994). The RuvB ATPase is the major engine in this pathway. Further elucidation of the mechanism by which RuvB couples ATP hydrolysis to DNA translocation and unwinding should help to clarify many aspects of these late stages in recombinational processes.

REFERENCES

Abrahams, J. P., Leslie, A. G., Lutter, R., & Walker, J. E. (1994) *Nature (London) 370*, 621−628.

Benson, F. E., Illing, G. T., Sharples, G. J., & Lloyd, R. G. (1988) *Nucleic Acids Res. 16*, 1541−1549.

Bujalowski, W., & Klonowska, M. M. (1993) *Biochemistry 32*, 5888−5900.

Bujalowski, W., Klonowska, M. M., & Jezewska, M. J. (1994) *J. Biol. Chem. 269*, 31350−31358.

Cleland, W. W. (1979) *Methods Enzymol. 63*, 500−513.

Davis, R. W., Botstein, D., & Roth, J. R. (1980) *Advanced Bacterial Genetics*, Cold Spring Harbor Laboratory, Cold Spring Harbor, NY.

Dean, F. B., & Hurwitz, J. (1991) *J. Biol. Chem. 266*, 5062−5071.

Dean, F. B., Borowiec, J. A., Eki, T., & Hurwitz, J. (1992) *J. Biol. Chem. 267*, 14129−14137.

Dong, F., Gogol, E. P., & von, H. P. (1995) *J. Biol. Chem. 270*, 7462−7473.

Egelman, E. H., Yu, X., Wild, R., Hingorani, M. M., & Patel, S. S. (1995) *Proc. Natl. Acad. Sci. U.S.A. 92*, 3869−3873.

Geiselmann, J., & von Hippel, P. H. (1992) *Protein Sci. 1*, 850−860.

Geiselmann, J., Seifried, S. E., Yager, T. D., Liang, C., & von Hippel, P. H. (1992a) *Biochemistry 31*, 121−132.

Geiselmann, J., Yager, T. D., Gill, S. C., Calmettes, P., & von Hippel, P. H. (1992b) *Biochemistry 31*, 111−121.

Hiom, K., & West, S. C. (1995) *Cell 80*, 787−793.

Iwasaki, H., Takahagi, M., Nakata, A., & Shinagawa, H. (1992) *Genes Dev. 6*, 2214−2220.

Iype, L. E., Wood, E. A., Inman, R. B., & Cox, M. M. (1994) *J. Biol. Chem. 269*, 24967−24978.

Iype, L. E., Inman, R. B., & Cox, M. M. (1995) *J. Biol. Chem. 270*, 19473−19480.

Kuzminov, A. (1993) *BioEssays 15*, 355−358.

Lloyd, R. G., & Sharples, G. J. (1993) *Nucleic Acids Res. 21*, 1719−1725.

Lohman, T. M. (1992) *Mol. Microbiol. 6*, 5−14.

Lohman, T. M. (1993) *J. Biol. Chem. 268*, 2269−2272.

Marrione, P. E., & Cox, M. M. (1995) *Biochemistry 34*, 9809−9818.

Messing, J. (1983) *Methods Enzymol. 101*, 20−78.

Mitchell, A. H., & West, S. C. (1994) *J. Mol. Biol. 243*, 208−215.

Morrical, S. W., Lee, J., & Cox, M. M. (1986) *Biochemistry 25*, 1482−1494.

Müller, B., & West, S. C. (1994) *Experientia 50*, 216−222.

Müller, B., Tsaneva, I. R., & West, S. C. (1993a) *J. Biol. Chem. 268*, 17179−17184.

Müller, B., Tsaneva, I. R., & West, S. C. (1993b) *J. Biol. Chem. 268*, 17185−17189.

Neuendorf, S. K., & Cox, M. M. (1986) *J. Biol. Chem. 261*, 8276−8282.

O'Sullivan, W. J., & Smithers, G. W. (1979) *Methods Enzymol. 63*, 294−336.

Parsons, C. A., Tsaneva, I., Lloyd, R. G., & West, S. C. (1992) *Proc. Natl. Acad. Sci. U.S.A. 89*, 5452−5456.

Parsons, C. A., Stasiak, A., Bennett, R. J., & West, S. C. (1995) *Nature (London) 374*, 375−378.

Patel, S. S., & Hingorani, M. M. (1995) *Biophys. J. 68* (*Suppl. 4*), 1865−1905.

Pedersen, P. L. (1994) *Curr. Biol. 4*, 1138−1141.

Senecoff, J. F., & Cox, M. M. (1986) *J. Biol. Chem. 261*, 7380−7386.

Shiba, T., Iwasaki, H., Nakata, A., & Shinagawa, H. (1991) *Proc. Natl. Acad. Sci. U.S.A. 88*, 8445−8449.

Shiba, T., Iwasaki, H., Nakata, A., & Shinagawa, H. (1993) *Mol. Gen. Genet. 237*, 395−399.

Shinagawa, H., Makino, K., Amemura, M., Kimura, S., Iwasaki, H., & Nakata, A. (1988) *J. Bacteriol. 170*, 4322−4329.

Shinagawa, H., Shiba, T., Iwasaki, H., Makino, K., Takahagi, M., & Nakata, A. (1991) *Biochimie 73*, 505−507.

Stasiak, A., Tsaneva, I. R., West, S. C., Benson, C. J., Yu, X., & Egelman, E. H. (1994) *Proc. Natl. Acad. Sci. U.S.A. 91*, 7618−7622.

Tsaneva, I. R., & West, S. C. (1994) *J. Biol. Chem. 269*, 26552−26558.

Tsaneva, I. R., Illing, G., Lloyd, R. G., & West, S. C. (1992a) *Mol. Gen. Genet. 235*, 1−10.

Tsaneva, I. R., Müller, B., & West, S. C. (1992b) *Cell 69*, 1171−1180.

Tsaneva, I. R., Müller, B., & West, S. C. (1993) *Proc. Natl. Acad. Sci. U.S.A. 90*, 1315−1319.

West, S. C., & Connolly, B. (1992) *Mol. Microbiol. 6*, 2755−2759.

West, S. C., Tsaneva, I. R., Hiom, K., & Benson, F. E. (1993) *Cold Spring Harbor Symp. Quant. Biol. 58*, 525−531.

Wong, I., & Lohman, T. M. (1992) *Science 256*, 350−355.

Wong, I., Chao, K. L., Bujalowski, W., & Lohman, T. M. (1992) *J. Biol. Chem. 267*, 7596−7610.

BI960316C